Experimental Investigation of Remote Coulomb Scattering on Mobility Degradation of Ge pMOSFET by Various PDA Ambiences

Lixing Zhou, Xiaolei Wang, Kai Han, Xueli Ma, Yanrong Wang, Jinjuan Xiang,
Hong Yang, Jing Zhang, Chao Zhao, Tianchun Ye, and Wenwu Wang

***Abstract*—The impact of various postdeposition annealing (PDA) ambiences (N_2, O_2, and NH_3) on the hole mobility of germanium (Ge) pMOSFET with GeO_2/Al_2O_3 gate-stack is investigated. It is found that the mobility is about 10% higher after N_2 PDA, while it is about 10% smaller after O_2 and NH_3 PDA than that without PDA. The physical origin is attributed to the remote Coulomb scattering. The Ge/GeO_2 interface charge Q_1 decreases, but the GeO_2/Al_2O_3 interface dipole Q_{dipole} increases after PDA in N_2, O_2, and NH_3. The higher mobility after N_2 PDA is due to a smaller Q_1 and Q_{dipole}, while the lower mobility after O_2 and NH_3 PDA is due to a larger Q_{dipole}. All these three PDA ambiences are beneficial to reduce the gate leakage current. Therefore, PDA in N_2 is a balance approach for both the hole mobility improvement and gate leakage current reduction.**

***Index Terms*—Dipole, gate leakage current, interfacial charges, mobility, postdeposition annealing (PDA).**

I. INTRODUCTION

GERMANIUM (Ge) is a very promising material because of its higher mobility for the application of Ge CMOS circuit [1], especially for Ge pMOSFET. The effective mobility, as a crucial parameter for device performance, suffers from several scattering mechanisms. Mobility is severely limited by surface roughness scattering at high normal field, and it can be improved by reducing the interface roughness or root mean square [2], [3]. Ge interface engineering has always been a key to achieve high-mobility MOSFET. On the one hand, a good interface quality can ensure a small-surface roughness [3], [4]. On the other hand, Coulomb scattering from the density of interface traps (D_{it}) can be greatly suppressed through sufficient passivation of Ge MOS interface [5]–[8] with a low D_{it} of 10^{11} $cm^{-2}\cdot eV^{-1}$ level. Forming gas annealing was used to improve the Ge/Al_2O_3 interface quality by inserting a GeO_2 interlayer (IL) [9], [10]. In addition, the hydrogen annealing induced out-diffusion of oxygen is also beneficial for mobility improvement by reducing the Coulomb scattering from the substrate oxygen atom [11]. References [12]–[14] have demonstrated that remote Coulomb scattering (RCS) from the gate-stack also plays an important role on the mobility degradation of Ge MOSFET. Three kinds of charges: Ge/IL interface charge, IL/high-κ interface charge, and IL/high-κ interface dipole, exist in the Ge gate-stack and deteriorate carrier mobility of Ge MOSFET [13], [14]. However, how these charges affect mobility is not comprehensively understood and still not clear.

In this paper, we first investigate the mobility change in various PDA ambiences (N_2, O_2, and NH_3) compared with that without annealing. Then, we analyze the change of the interfacial charges and dipole in Ge gate-stack induced by PDA. These results show that various PDA ambiences have different effects on the fixed charges and dipole, and cause the mobility variation. In addition, we also investigate the effect of PDA on gate leakage current. The result shows that N_2 annealing is beneficial for both the mobility and gate leakage current improvement.

II. EXPERIMENT

First, Ge MOSFET was fabricated. After the n-type Ge substrate ($\sim 1.6 \times 10^{15}$ cm^{-3}) cleaning by diluted HF, the GeO_2/Al_2O_3 gate-stack was deposited immediately in atomic layer deposition (ALD) chamber. GeO_2 by ozone oxidation was grown at 300 °C for 25 min. The 7-nm Al_2O_3 was deposited using trimethylaluminium and H_2O as precursors at 300 °C. One sample without annealing was as the control sample. The others went through PDA in N_2, O_2, and NH_3 ambiences at 400 °C for 30 min. Al was used as the gate electrode by e-beam evaporation. The boron ion was implanted using an energy of 5 keV with a dose of 10^{15} cm^{-2},

Manuscript received January 17, 2019; revised February 15, 2019; accepted February 19, 2019. This work was supported in part by the National Natural Science of China under Grant 61574168, Grant 61504163, and Grant 61674003, and in part by the National High Technology Research and Development Program 863 of China under Grant 2015AA010601. The review of this paper was arranged by Editor R. Wang. *(Corresponding authors: Xiaolei Wang; Kai Han; Wenwu Wang.)*

L. Zhou, X. Wang, X. Ma, J. Xiang, H. Yang, C. Zhao, T. Ye, and W. Wang are with the Key Laboratory of Microelectronics Devices and Integrated Technology, Institute of Microelectronics, Chinese Academy of Sciences, Beijing 100029, China, and also with the School of Electronic, Electrical and Communication Engineering, University of Chinese Academy of Sciences, Beijing 100049, China (e-mail: wangxiaolei@ime.ac.cn; wangwenwu@ime.ac.cn).

K. Han is with the School of Physics and Optoelectronic Engineering, Weifang University, Weifang 261061, China (e-mail: hankai@wfu.edu.cn).

Y. Wang and J. Zhang are with the Microelectronics Department, North China University of Technology, Beijing 100041, China.

Color versions of one or more of the figures in this paper are available online at http://ieeexplore.ieee.org.

Digital Object Identifier 10.1109/TED.2019.2900801

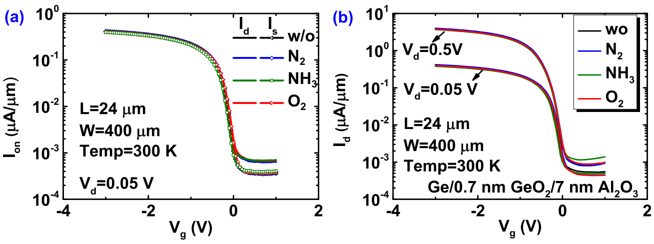

Fig. 1. I_d–V_g characteristics of Ge pMOSFET for various PDA ambiences at 300 K.

following which activation annealing was performed at 400 °C for 1 min in N_2. Finally, a Ni source/drain contact was formed by e-beam evaporation.

Second, Ge MOS capacitor was fabricated. The gate structures grown by ALD with the same Al_2O_3 and different GeO_2 thicknesses, and the same GeO_2 and different Al_2O_3 thicknesses, namely, the terraced GeO_2 and Al_2O_3 structures, were used. For the terraced GeO_2 structure, GeO_2 with ozone oxidation was grown at 300 °C, 350 °C, and 400 °C for 25 min in ALD chamber to obtained different GeO_2 thicknesses [15]; the 10-nm Al_2O_3 was formed on GeO_2. For the terraced Al_2O_3 structure, GeO_2 was grown at 300 °C and different Al_2O_3 thicknesses (5, 10, 15, and 20 nm) was formed on GeO_2. One sample with the terraced GeO_2 and Al_2O_3 structures had no PDA process. The others went through PDA in N_2, O_2, and NH_3 ambiences at 400 °C for 30 min. Al was used as the gate electrode by e-beam evaporation. The terraced GeO_2 and Al_2O_3 structures were aimed to extract the interfacial charges. Here, the dielectrics with large physical thicknesses were used. It can be a way to ensure the mobility extraction only from the carrier inversion and reduce the interference from the gate leakage. In addition, using large physical thickness helps make a more obvious thickness gradient to improve the accuracy of experimentally extracted charges [16]. To investigate the gate leakage current, a group of GeO_2/Al_2O_3 gate-stack MOS capacitors without and with N_2, O_2, and NH_3 PDA were fabricated. GeO_2 was grown at 300 °C for 25-min, and 4-nm Al_2O_3 was deposited in the ALD chamber. Al was a gate electrode.

XPS measurement was performed. The 0.7-nm GeO_2 was grown by ozone oxidation on the clean Ge surface, and 2-nm Al_2O_3 was then deposited on GeO_2. One sample was as the reference sample and the others went through annealing in N_2, O_2, and NH_3 ambiences at 400 °C for 30 min. The XPS measurement was performed using Thermo Scientific ESCALAB 250xi equipped with a monochromatic Al Kα radiation source. The pass energy was set as 15 eV. All of the data were collected at a takeoff angle of 90° relative to the sample surface.

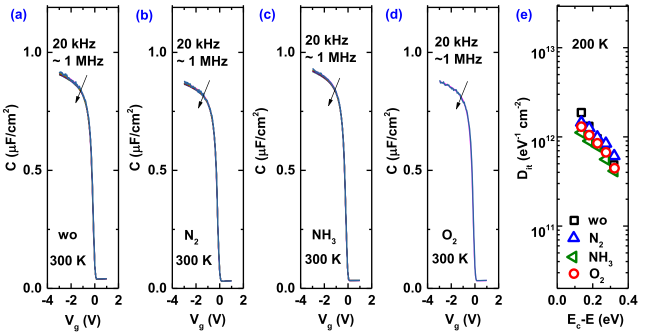

Fig. 2. Gate-to-channel capacitance (C_{gc}) plots of Ge pMOSFET (a) without PDA and with PDA in (b) N_2, (c) NH_3, and (d) O_2. (e) D_{it} for different PDA ambiences.

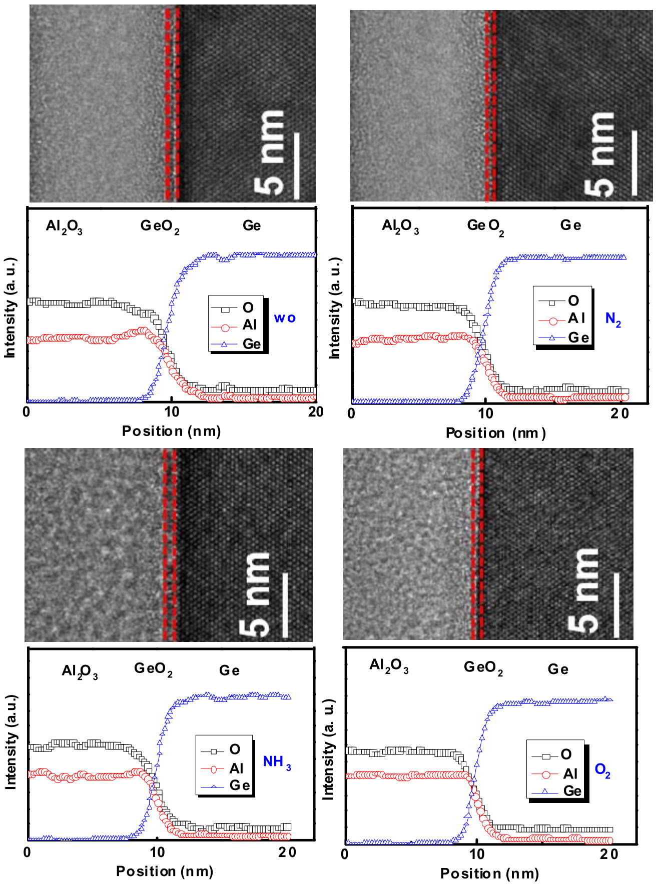

Fig. 3. TEM images and EDS depth profiles for Ge/GeO_2/Al_2O_3 structure without PDA and with PDA in N_2, O_2, and NH_3.

III. RESULTS AND DISCUSSION

A. Hole Mobility for Different PDA Ambiences

Fig. 1(a) shows the drain and source current at a drain voltage of 0.05 V, and Fig. 1(b) shows the I_d–V_g characteristics at two drain voltages of 0.05 and 0.5 V for various PDA ambiences at 300 K. The larger drain OFF-state current is due to the graded p-n junction between the drain region and channel. According to the source current, the ratio of the I_{ON}/I_{OFF} is about 1×10^3, and the subthreshold swing (SS) is 142 mV/dec. The effective region of inversion carrier concentration Ns for mobility extraction begins with 1×10^{12} cm^{-2} which is over the OFF-state region, and the result of 1×10^3 ON–OFF ratio can satisfy our experimental requirement for mobility analysis. From Fig. 1, I_d increases slightly in N_2, while it is decreases in O_2 and NH_3 compared with the I_d without PDA. Fig. 2 shows the C_{gc}–V_g characteristics at multiple frequencies and the D_{it} for various PDA ambiences. Well C–V plot indicates good interface quality. The D_{it} was obtained by the low-temperature

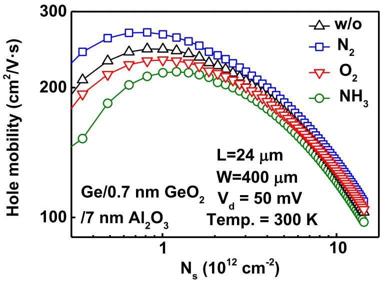

Fig. 4. Hole mobility versus N_S of Ge pMOSFET at 300 K in various PDA ambiences.

conductance method. All the PDA samples have almost the same D_{it}. In addition, the nearly coincident C–V curves at the depletion region indicate that the Ge/GeO$_2$ interface quality keeps unchanged for different PDA ambiences. Moreover, the SS in Fig. 1 also indicates no difference of the Ge/GeO$_2$ interface quality among various PDA ambiences.

Fig. 3 shows the transmission electron microscope (TEM) images and energy dispersive spectrometer (EDS) depth profiles for Ge/GeO$_2$/Al$_2$O$_3$ structure without PDA and with PDA in N$_2$, O$_2$, and NH$_3$. PDA does not change the physical thickness of the gate dielectrics. EDS results show that O, Ge, and Al elements have almost the same trend after PDA. The not exact match among all the PDA curves is due to the measurement error. There is no GeO$_2$ regrowth after PDA. The maximum C_{gc} successively increases for the N$_2$, O$_2$, without, and NH$_3$ annealing samples. The maximum of $C_{gc}$is different after PDA in N$_2$, NH$_3$, and O$_2$. This phenomenon can be attributed to the dielectric constant change induced by different ambiences. Although the very low level of the introduced atoms, the interaction between them and the dielectric may still change the value of the dielectric constant and the maximum of the capacitance. Hole mobility is extracted by split C–V, as shown in Fig. 4. The mobility has an obvious variation among different PDA ambiences. Compared to the sample without PDA, the hole mobility increases in N$_2$, while it decreases in O$_2$ and NH$_3$.

This mobility change is investigated from the viewpoint of the scattering mechanism. First, we consider the phonon scattering. Because we use the same substrate material and measure the I_d and C_{gc} at the same temperature, the phonon scattering should have the same effect on mobility and not be responsible for the mobility variation in different ambiences. Second, the surface roughness scattering is dominant in the region of high inversion charges (N_s) [3], [17]. Moreover, from the HRTEM results, as shown in Fig. 3, there is no difference at the Ge/GeO$_2$ interface after PDA. Therefore, the PDA does not affect the interface quality and surface roughness. Third, we consider the Coulomb scattering from the D_{it}. We have demonstrated a D_{it} of $3 \times 10^{11}\ \mathrm{eV}^{-1}\cdot\mathrm{cm}^{-2}$ for a GeO$_2$ thickness of 0.7 nm [14], [18]. The D_{it} is almost the same for all the PDA samples, and it has the same scattering effect on the mobility. The same D_{it} for all the samples could not explain the mobility change after different PDA ambiences. The mobility change is induced by the gate charges in the gate-stack. For the GeO$_2$/Al$_2$O$_3$ gate-stack, the RCS from the fixed charges at the Ge/GeO$_2$ and GeO$_2$/Al$_2$O$_3$ interfaces and dipole at the GeO$_2$/Al$_2$O$_3$ interface degrades the mobility of Ge MOSFET [13], [14]. The change of these charges in the gate-stack by PDA is a possible reason for the mobility variation. In the following, we investigate the RCS.

B. Charge Distribution for Different PDA Ambiences

The RCS is strongly correlated with the charge distribution in gate-stack. Thus, we first experimentally explore the charge distribution in the Ge gate-stack after PDA in various ambiences. We obtained the interfacial charges from the relationship between the flat voltage (V_{FB}) and equivalent oxide thickness (EOT) of MOS capacitors. The V_{FB} was obtained from the shift by fitting the experimental and theoretical C–V curves considering the quantum effect. In this paper, we fabricated MOS capacitors with different GeO$_2$ thicknesses and the same Al$_2$O$_3$ thickness. For the terraced GeO$_2$ structure, the MOS capacitor has a group of values of V_{FB} and EOT for each GeO$_2$ thickness. Then, several groups of V_{FB} and EOT can be obtained from the C–V curves of MOS capacitors with different GeO$_2$ thicknesses. The relationship between V_{FB} and EOT for the Al/Al$_2$O$_3$/terraced GeO$_2$/Ge MOS capacitor can be described as

$$\begin{aligned} V_{FB} = &-\frac{Q_1}{\varepsilon_0\varepsilon_r}\mathrm{EOT} - \frac{\varepsilon_1\rho_1}{2\varepsilon_0\varepsilon_r^2}\mathrm{EOT}^2 \\ &-\frac{Q_2}{\varepsilon_0\varepsilon_r}\mathrm{EOT}_2 + \frac{(\varepsilon_1\rho_1 - \varepsilon_2\rho_2)}{2\varepsilon_0\varepsilon_r^2}\mathrm{EOT}_2^2 + \Delta + \phi_{ms} \end{aligned} \quad (1)$$

where Q_1 is the areal charge at the GeO$_2$/Ge interface, Q_2 is the areal charge at the Al$_2$O$_3$/GeO$_2$ interface, ρ_1 is the bulk charge density in GeO$_2$, ρ_2 is the bulk charge density in Al$_2$O$_3$, ε_0 is the vacuum permittivity, ε_r is the relative permittivity of SiO$_2$, ε_1 is the relative permittivity of GeO$_2$, ε_2 is the relative permittivity of Al$_2$O$_3$, EOT is the equivalent oxide thickness of the whole gate-stacks, EOT$_2$ is the equivalent oxide thickness of the Al$_2$O$_3$ dielectric, Δ means V_{FB} shift due to the electric dipole at the Al$_2$O$_3$/GeO$_2$ interface, and ϕ_{ms} is the vacuum work function difference between the Al gate electrode and Ge substrate. Similarly, we fabricated MOS capacitors with different Al$_2$O$_3$ thicknesses and the same GeO$_2$ thickness. For each Al$_2$O$_3$ thickness, the V_{FB} and the corresponding EOT can be acquired from the C–V measurement. When Al$_2$O$_3$ thickness varies, several groups of V_{FB} and EOT can be obtained from the C–V curves of MOS capacitors for the terraced Al$_2$O$_3$ structure. The relationship between V_{FB} and EOT for the Al/terraced Al$_2$O$_3$/GeO$_2$/Ge MOS capacitor can be described as

$$\begin{aligned} V_{FB} = &-\frac{Q_1+Q_2}{\varepsilon_0\varepsilon_r}\mathrm{EOT} + \frac{\varepsilon_2\rho_2\mathrm{EOT}_1}{\varepsilon_0\varepsilon_r^2}\mathrm{EOT} - \frac{\varepsilon_2\rho_2}{2\varepsilon_0\varepsilon_r^2}\mathrm{EOT}^2 \\ &+\frac{Q_2\mathrm{EOT}_1}{\varepsilon_0\varepsilon_r} - \frac{\varepsilon_2\rho_2}{2\varepsilon_0\varepsilon_r^2}\mathrm{EOT}_1^2 + \Delta + \phi_{ms} \end{aligned} \quad (2)$$

where EOT$_1$ is the equivalent oxide thickness of the GeO$_2$ dielectric.

Fig. 5(a) and (b) shows the V_{FB}–EOT plots of the terraced GeO$_2$ and Al$_2$O$_3$ structures for the samples without and with PDA in N$_2$, O$_2$, and NH$_3$ ambiences. A linear relationship

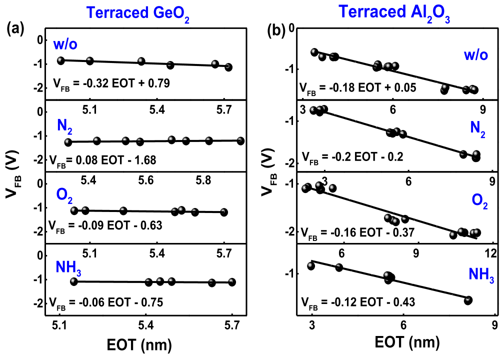

Fig. 5. V_{FB} versus EOT plots of the (a) Ge/terraced GeO$_2$/Al$_2$O$_3$/Al and (b) Ge/GeO$_2$/terraced Al$_2$O$_3$/Al structures for the without and with annealing samples in N$_2$, O$_2$, and NH$_3$.

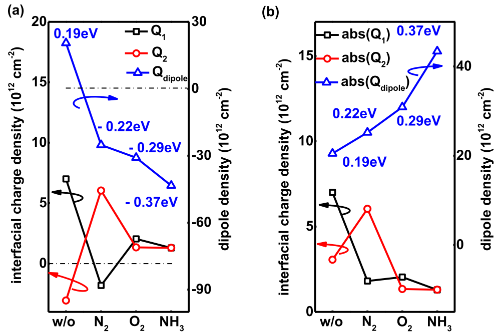

Fig. 6. (a) Charge values with the respective polarity and (b) charge absolute value of the interfacial and dipole charges in the Ge gate-stack.

between V_{FB} and EOT can be observed from all the samples. Bulk charge ρ_1 and ρ_2 in GeO$_2$ and Al$_2$O$_3$ are negligible. Therefore, the fixed charge Q_1 at the Ge/GeO$_2$ interface is obtained from the slope of (1). The fixed charge Q_2 at the GeO$_2$/Al$_2$O$_3$ interface is obtained from the slope of (2) subtracting the Q_1. The dipole Q_{dipole} at the GeO$_2$/Al$_2$O$_3$ interface can be obtained from the intercept of (1) or (2). The dipole at GeO$_2$/Al$_2$O$_3$ interface may be modeled by a parallel-plate capacitor with an effective thickness T_{eff}. The T_{eff} is the inner distance between the positive and negative charges of the dipole which is taken as ~0.3 nm [19], [20]. The charge distribution is shown in Fig. 6 for different PDA ambiences. Fig. 6(a) shows the charge distribution with the polarity change for various PDA ambiences: both the quantity and polarity of the interfacial charges and dipole change after PDA. The polarity of Q_1 becomes negative in N$_2$, Q_2 becomes positive, and Q_{dipole} becomes negative in N$_2$, O$_2$, and NH$_3$ compared with the sample without annealing. Because the RCS only depends on the charge quantity but not on the polarity, thus, we compare the absolute charge value, as shown in Fig. 6(b). The charge density Q_1 decreases after PDA in N$_2$, O$_2$, and NH$_3$, Q_2 increases in N$_2$ while the decrease in O$_2$ and NH$_3$, and Q_{dipole} increases in N$_2$, O$_2$, and NH$_3$ compared with the sample without annealing. The dipole density is almost one order of magnitude larger than Q_1 and Q_2.

The dipole is also confirmed from the XPS spectra. Fig. 7 records the Ge 3d and Al 2p spectra with and without PDA. There is no obvious change of the GeO$_2$ intensity. It can be seen that N$_2$, O$_2$, and NH$_3$ annealing makes the peak position of Ge 3d$^{\mathrm{GeO2}}$ and Al 2p$^{\mathrm{Al2O3}}$ shift to a lower binding energy.

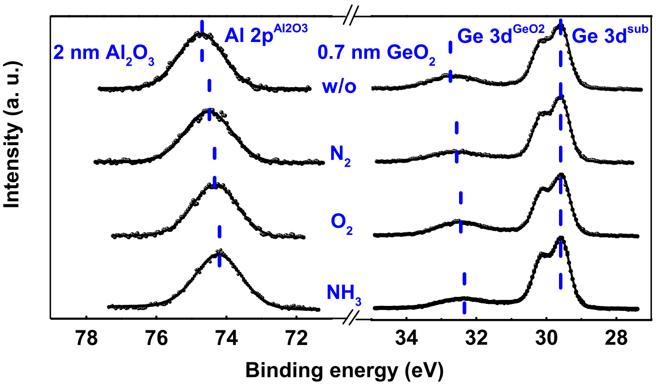

Fig. 7. Ge 3d and Al 2p spectra of samples with Al$_2$O$_3$/GeO$_2$/Ge structure without and with PDA in N$_2$, O$_2$, and NH$_3$ ambiences.

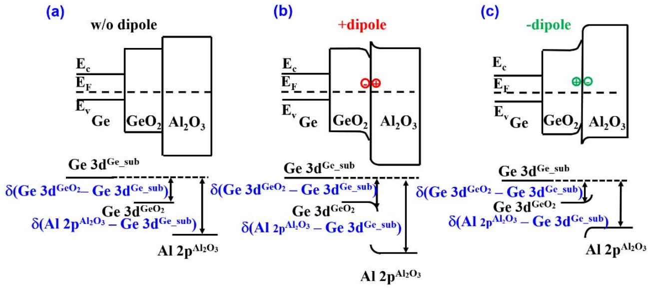

Fig. 8. Schematic band diagrams for Al$_2$O$_3$/GeO$_2$/Ge stacks (a) without dipole, (b) with positive dipole, and (c) with negative dipole at the Al$_2$O$_3$/GeO$_2$ interface.

These results also show a dipole at the GeO$_2$/Al$_2$O$_3$interface, which can cause the GeO$_2$ and Al$_2$O$_3$ band bending at the interface, and therefore, result in the shift of GeO$_2$ and Al$_2$O$_3$ core level. The successively larger shift of Ge 3d$^{\mathrm{GeO2}}$ and Al 2p$^{\mathrm{Al2O3}}$ binding energy in N$_2$, O$_2$, and NH$_3$ also shows a larger and larger dipole at the GeO$_2$/Al$_2$O$_3$ interface. The XPS results are consistent with the dipole change in Fig. 6. The reason can be explained, as shown in Fig. 8. A positive dipole induces decreased Al$_2$O$_3$ energy band level. At the same time, the energy band bends downward and upward in the GeO$_2$ and Al$_2$O$_3$ side, respectively. Therefore, the distance between Ge 3d$^{\mathrm{GeO2}}$ and Ge 3d$^{\mathrm{Ge_sub}}$$\delta$(Ge 3d$^{\mathrm{GeO2}}$–Ge 3d$^{\mathrm{Ge_sub}}$) and distance between Al 2p$^{\mathrm{Al2O3}}$ and Ge 3d$^{\mathrm{Ge_sub}}$$\delta$(Al 2p$^{\mathrm{Al2O3}}$–Ge 3d$^{\mathrm{Ge_sub}}$) increase. A negative dipole induces increased Al$_2$O$_3$ energy band level. At the same time, the energy band bends upward and downward in the GeO$_2$ and Al$_2$O$_3$ side, respectively. Therefore, the core level shift δ(Ge 3d$^{\mathrm{GeO2}}$–Ge 3d$^{\mathrm{Ge_sub}}$) and δ(Al 2p$^{\mathrm{Al2O3}}$–Ge 3d$^{\mathrm{Ge_sub}}$) decrease. The larger the negative dipole, the smaller the δ(Ge 3d$^{\mathrm{GeO2}}$–Ge 3d$^{\mathrm{Ge_sub}}$) and δ(Al 2p$^{\mathrm{Al2O3}}$–Ge 3d$^{\mathrm{Ge_sub}}$) are. A more detailed explanation for the dipole formation can be found elsewhere [21].

C. RCS for Different PDA Ambiences

There are three kinds of charges in the Al$_2$O$_3$/GeO$_2$/Ge gate-stacks, including the Ge/GeO$_2$ interface charge Q_1, GeO$_2$/Al$_2$O$_3$ interface charge Q_2, and interface dipole Q_{dipole}. First, we discuss the effect of the Ge/GeO$_2$ interface charge Q_1. The mobility limited by the Coulomb scattering from Q_1 is proportional to $1/Q_1$ [24], [25]. The mobility will degrade with increased fixed charges at the Ge/GeO$_2$ interface. The value of Q_1 after PDA in N$_2$, O$_2$, and NH$_3$ is much

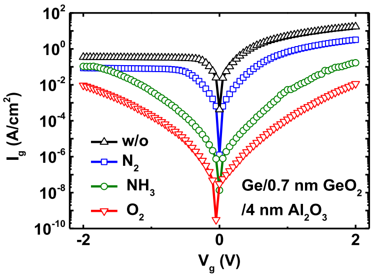

Fig. 9. Gate leakage current as a function of gate voltage for Ge/0.7-nm GeO_2/4-nm Al_2O_3/Al capacitors for various PDA ambiences.

smaller than that without annealing. This indicates that the Coulomb scattering from Q_1 is sufficiently suppressed by PDA. However, we observe the mobility increasing in N_2 and decreasing in O_2 and NH_3. The mobility must be affected by the charges at the GeO_2/Al_2O_3 interface. Second, we consider the effect of the GeO_2/Al_2O_3 interface charge Q_2 and Q_{dipole}. The GeO_2/Al_2O_3 interface charge Q_2 and dipole Q_{dipole} have the same physical distance from the channel surface. However, the Q_{dipole} ($\sim 10^{13}$ cm^{-2}) is an order of magnitude greater than Q_2 ($\sim 10^{12}$ cm^{-2}), and it has a more remarkable effect on the mobility degradation than Q_2. The RCS rate is proportional to the fixed charge density in the gate-stack [22], [23]. The amount of dipole is a key factor to determine the mobility. The mobility should decrease with the fixed charge density since the RCS potential increases, i.e., RCS increases. The dipole moment increases from 0.19 eV without annealing to 0.22, 0.29, and 0.37 eV after PDA in N_2, O_2, and NH_3, respectively. The increased dipole will scatter carrier more severely. N_2 can increase mobility, while O_2 and NH_3 reduce mobility as a joint result of Ge/GeO_2 interface Q_1 and GeO_2/Al_2O_3 interface Q_{dipole}. N_2 improves the mobility because of the much lower Q_1. The reduction of Q_1 has a major responsibility for the mobility improvement. However, although a remarkable reduction of Q_1 in O_2 and NH_3, the mobility still shows a decline which is due to an enormous increase of dipole. Therefore, the dipole plays an important role on the mobility degradation. N_2 annealing is helpful to the mobility promotion.

D. Gate Leakage for Different PDA Ambiences

To analyze the changes of gate leakage current I_g after PDA, we measured I_g from different devices with Ge/0.7-nm GeO_2/4-nm Al_2O_3/Al structure. Fig. 9 shows the gate leakage current variation in different PDA ambiences. It can be seen that the gate leakage current displays an obvious improvement after PDA. The leakage current in N_2 is one order of magnitude smaller than that of the sample without PDA. NH_3 and O_2 PDA make a more excellent gate leakage current performance, which is 10^3–10^4 lower than that of the without PDA sample. Fig. 6 indicates a reduction of fixed charges at the Ge/GeO_2 interface, which may contribute to the improvement of gate leakage current. The gate current is closely related to the interfacial defect [12], [26], [27]. For the GeO_2 IL by ozone oxidation, we obtained positive charges at the Ge/GeO_2 interface. Our previous report [28] demonstrated that the positive charge is due to the oxygen vacancy. An amount of defect induced by oxygen vacancy exists at the Ge/GeO_2 interface, and grade in the bulk GeO_2. The gate leakage current can be affected by the oxygen vacancy due to the charge trap and detrap. The IL thickness is verified by HRTEM. The GeO_2 thickness does not change after PDA. Therefore, the passivation of oxygen vacancy at the Ge/GeO_2 interface is responsible for the gate leakage current improvement after PDA. O_2 annealing has a much better passivation of oxygen vacancy and reduces the gate leakage current. These results demonstrate the importance of PDA to reduce the gate leakage current and improve the MOS capacitor performance.

IV. CONCLUSION

We demonstrated the effect of PDA ambiences on the mobility of Ge pMOSFET and gate leakage current of Ge MOS capacitor. The mobility variation results from the interfacial charge and dipole change induced by various PDA ambiences. N_2 PDA is beneficial but O_2 and NH_3 PDA are detrimental to the mobility improvement. However, the three PDA ambiences are all helpful to reduce the gate leakage current. N_2 annealing is a balance approach for the mobility promotion and gate leakage current reduction.

REFERENCES

[1] S. Shin *et al.*, “Performance potential of Ge CMOS technology from a material-device-circuit perspective,” *IEEE Trans. Electron Devices*, vol. 65, no. 5, pp. 1679–1684, May 2018. doi: 10.1109/TED.2018.2816576.

[2] N. Taoka, W. Mizubayashi, Y. Morita, S. Migita, H. Ota, and S. Takagi, “Physical origins of mobility enhancement of Ge p-channel metal-insulator-semiconductor field effect transistors with Si passivation layers,” *J. Appl. Phys.*, vol. 108, no. 10, Nov. 2010, Art. no. 104511. doi: 10.1063/1.3512868.

[3] R. Zhang, X. Yu, M. Takenaka, and S. Takagi, “Physical origins of high normal field mobility degradation in Ge p- and n-MOSFETs with GeO_x/Ge MOS interfaces fabricated by plasma postoxidation,” *IEEE Trans. Electron Devices*, vol. 61, no. 7, pp. 2316–2323, Jul. 2014. doi: 10.1109/ted.2014.2325604.

[4] Y. Oniki, H. Koumo, Y. Iwazaki, and T. Ueno, “Evaluation of GeO desorption behavior in the metalGeO_2/Ge structure and its improvement of the electrical characteristics,” *J. Appl. Phys.*, vol. 107, no. 12, Jun. 2010, Art. no. 124113. doi: 10.1063/1.3452367.

[5] C. H. Lee *et al.*, “Ge MOSFETs performance: Impact of Ge interface passivation,” in *IEDM Tech. Dig.*, Dec. 2010, pp. 18.1.1–18.1.4. doi: 10.1109/IEDM.2010.5703384.

[6] R. Zhang, X. Yu, M. Takenaka, and S. Takagi, “Impact of postdeposition annealing ambient on the mobility of Ge nMOSFETs with 1-nm EOT Al_2O_3/GeO_x/Ge gate-stacks,” *IEEE Trans. Electron Devices*, vol. 63, no. 2, pp. 558–564, Feb. 2016. doi: 10.1109/ted.2015.2509961.

[7] R. Zhang, X. Tang, X. Yu, J. Li, and Y. Zhao, “Aggressive EOT scaling of Ge pMOSFETs with $HfO_2/AlO_x/GeO_x$ gate-stacks fabricated by ozone postoxidation,” *IEEE Electron Device Lett.*, vol. 37, no. 7, pp. 831–834, Jul. 2016. doi: 10.1109/led.2016.2572731.

[8] C. H. Lee, T. Nishimura, K. Nagashio, K. Kita, and A. Toriumi, “High-electron-mobilityGe/GeO_2 n-MOSFETs with two-step oxidation,” *IEEE Trans. Electron Devices*, vol. 58, no. 5, pp. 1295–1301, May 2011. doi: 10.1109/ted.2011.2111373.

[9] L. Zhang *et al.*, “Selective passivation of GeO_2/Ge interface defects in atomic layer deposited high-k MOS structures,” *ACS Appl. Mater. Interfaces*, vol. 7, no. 37, pp. 20499–20506, Sep. 2015. doi: 10.1021/acsami.5b06087.

[10] S. Swaminathan, Y. Sun, P. Pianetta, and P. C. McIntyre, “Ultrathin ALD-Al_2O_3 layers for Ge(001) gate stacks: Local composition evolution and dielectric properties,” *J. Appl. Phys.*, vol. 110, no. 9, Nov. 2011, Art. no. 094105. doi: 10.1063/1.3647761.

[11] C. H. Lee, T. Nishimura, C. Lu, S. Kabuyanagi, and A. Toriumi, "Dramatic effects of hydrogen-induced out-diffusion of oxygen from Ge surface on junction leakage as well as electron mobility in n-channel Ge MOSFETs," in *IEDM Tech. Dig.*, Dec. 2014, pp. 32.5.1–32.5.4. doi: 10.1109/IEDM.2014.7047156.

[12] R. Zhang, T. Iwasaki, N. Taoka, M. Takenaka, and S. Takagi, "High-mobility Ge pMOSFET with 1-nm EOT Al_2O_3/GeO_x/Ge gate stack fabricated by plasma post oxidation," *IEEE Trans. Electron Devices*, vol. 59, no. 2, pp. 335–341, Feb. 2012. doi: 10.1109/ted.2011.2176495.

[13] L. Zhou *et al.*, "Hole mobility degradation by remote Coulomb scattering and charge distribution in Al_2O_3/GeO_x gate stacks in bulk Ge pMOSFET with GeO_x grown by ozone oxidation," *J. Phys. D, Appl. Phys.*, vol. 50, no. 24, May 2017, Art. no. 245102. doi: 10.1088/1361-6463/aa6f96.

[14] X. Wang *et al.*, "Remote interfacial dipole scattering and electron mobility degradation in Ge field-effect transistors with GeO_x/Al_2O_3 gate dielectrics," *J. Phys. D, Appl. Phys.*, vol. 49, no. 25, May 2016, Art. no. 255104. doi: 10.1088/0022-3727/49/25/255104.

[15] X. Wang *et al.*, "Experimental investigation on oxidation kinetics of germanium by ozone," *Appl. Surf. Sci.*, vol. 390, pp. 472–480, Dec. 2016. doi: 10.1016/j.apsusc.2016.08.123.

[16] X. Wang *et al.*, "Comprehensive understanding of the effect of electric dipole at high-k/SiO_2 interface on the flatband voltage shift in metal-oxide-semiconductor device," *Appl. Phys. Lett.*, vol. 97, no. 6, Aug. 2010, Art. no. 062901. doi: 10.1063/1.3475774.

[17] S. Takagi, A. Toriumi, M. Iwase, and H. Tango, "On the universality of inversion layer mobility in Si MOSFET's: Part I-effects of substrate impurity concentration," *IEEE Trans. Electron Devices*, vol. 41, no. 12, pp. 2357–2362, Dec. 2002. doi: 10.1109/16.337449.

[18] X. Wang, J. Xiang, W. G. Wang, Y. Xiong, J. Zhang, and C. Zhao, "Investigation on the dominant key to achieve superior Ge surface passivation by GeOx based on the ozone oxidation," *Appl. Surf. Sci.*, vol. 357, pp. 1857–1862, Dec. 2015. doi: 10.1016/j.apsusc.2015.09.084.

[19] W. Mönch, *Semiconductor Surfaces and Interfaces*, 3rd ed. Berlin, Germany: Springer-Verlag, 2001, p. 92.

[20] S. G. Louie, J. R. Chelikowsky, and M. L. Cohen, "Ionicity and the theory of Schottky barriers," *Phys. Rev. B, Covering Condens. Matter Mater. Phys.*, vol. 15, no. 4, pp. 2154–2162, Feb. 1977. doi: 10.1103/PhysRevB.15.2154.

[21] L. Zhou *et al.*, "Understanding dipole formation at dielectric/dielectric hetero-interface," *Appl. Phys. Lett.*, vol. 113, no. 18, Nov. 2018, Art. no. 181601. doi: 10.1063/1.5049423.

[22] S.-I. Saito *et al.*, "Remote-charge-scattering limited mobility in field-effect transistors with SiO_2 and Al_2O_3/SiO_2 gate stacks," *J. Appl. Phys.*, vol. 98, no. 11, Dec. 2005, Art. no. 113706. doi: 10.1063/1.2135878.

[23] H. Ota *et al.*, "Intrinsic origin of electron mobility reduction in high-k MOSFETs—From remote phonon to bottom interface dipole scattering," in *IEDM Tech. Dig.*, pp. 65–68, Dec. 2007. doi: 10.1109/IEDM.2007.4418864.

[24] M. V. Haartman *et al.*, "Low-frequency noise and Coulomb scattering in $Si_{0.8}Ge_{0.2}$ surface channel pMOSFETs with ALD Al_2O_3 gate dielectrics," *Solid-State Electron.*, vol. 49, no. 6, pp. 907–914, Jun. 2005. doi: 10.1016/j.sse.2005.03.009.

[25] S. C. Sun and J. D. Plummer, "Electron mobility in inversion and accumulation layers on thermally oxidized silicon surfaces," *IEEE J. Solid-State Circuits*, vol. 15, no. 4, pp. 562–573, Aug. 1980. doi: 10.1109/T-ED.1980.20063.

[26] N. Wu *et al.*, "Effect of surface NH_3 anneal on the physical and electrical properties of HfO_2 films on Ge substrate," *Appl. Phys. Lett.*, vol. 84, pp. 3741–3743, Apr. 2004. doi: 10.1063/1.1737057.

[27] W. P. Bai *et al.*, "Ge MOS characteristics with CVD HfO_2 gate dielectrics and TaN gate electrode," in *Dig. Tech. Papers-Symp. VLSI Technol.*, Oct. 2003, pp. 121–122. doi: 10.1109/vlsit.2003.1221115.

[28] L. Zhou *et al.*, "Identification of interfacial defects in a Ge gate stack based on ozone passivation," *Semicond. Sci. Technol.*, vol. 33, no. 11, Oct. 2018, Art. no. 115005. doi: 10.1088/1361-6641/aae006.